Basic & Clinical Pharmacology & Toxicology

BCPT Basic & Clinical Pharmacology & Toxicology

ORIGINAL ARTICLE OPEN ACCESS

Bruceine A Inhibits Cell Proliferation by Targeting the USP13/PARP1 Signalling Pathway in Multiple Myeloma

Mengjie Guo[1,2] | Han Meng[2] | Yi Sun[2] | Lianxin Zhou[2] | Tingting Hu[2] | Tianyi Yu[2] | Haowen Bai[2] | Yuanjiao Zhang[2] | Chunyan Gu[1,2] | Ye Yang[2]

[1]Nanjing Hospital of Chinese Medicine Affiliated With Nanjing University of Chinese Medicine, Nanjing, China | [2]School of Medicine, Nanjing University of Chinese Medicine, Nanjing, China

Correspondence: Yuanjiao Zhang (13770552470@163.com) | Chunyan Gu (guchunyan@njucm.edu.cn) | Ye Yang (yangye876@sina.com)

Received: 18 November 2024 | **Revised:** 21 February 2025 | **Accepted:** 10 March 2025

Funding: This work was supported by National Natural Science Foundation of China 82304599, Scientific Research Foundation of Nanjing University of Chinese Medicine (013091007003-1) (to YZ) and the Priority Academic Program Development of Jiangsu Higher Education Institutions (Integration of Chinese and Western Medicine).

Keywords: Bruceine A | DNA damage repair | multiple myeloma | PARP1 | USP13

ABSTRACT

Multiple myeloma (MM) is an incurable hematologic malignancy, driving significant interest in the discovery of novel therapeutic strategies. Bruceine A (BA), a tetracyclic triterpene quassinoid derived from *Brucea javanica*, has shown anticancer properties by modulating multiple intracellular signalling pathways and exhibiting various biological effects. However, the specific pharmacological mechanisms by which it combats MM remain unclear. In this study, we identified USP13 as a potential target of BA. We observed a significant increase in USP13 expression in patients with MM, which was strongly associated with a poorer prognosis. Furthermore, enhanced USP13 expression can stimulate MM cell proliferation both in vitro and in vivo. Mass spectrometry analysis, combined with co-immunoprecipitation and in vitro ubiquitination experiments, revealed PARP1 as a critical downstream target of USP13. USP13 can stabilize PARP1 protein through deubiquitination, promoting PARP1-mediated DNA damage repair (DDR) and facilitating MM progression. Notably, we utilized MM cell lines, an MM Patient-Derived Tumour Xenograft model, and a 5TMM3VT mouse model to determine the anticancer effects of BA on MM progression, revealing its potential to target USP13/PARP1 signalling and disrupt DDR in MM cells. In conclusion, these findings suggest that BA inhibiting USP13/PARP1-mediated DDR might be a promising therapeutic strategy for MM.

1 | Introduction

Multiple myeloma (MM) is an incurable and heterogeneous haematological malignancy defined by abnormal clonal expansion of malignant plasma cells in the bone marrow [1]. Recent progress in therapeutic approaches, such as proteasome inhibitors (PIs), immunomodulatory drugs and monoclonal antibodies, have contributed to better overall and event-free survival rates [2]. Nevertheless, patients frequently encounter relapses and develop resistance to existing treatments, resulting in progressively shorter periods of remission [2]. Therefore, it is crucial to identify new therapeutic targets and develop potent drugs that can overcome drug resistance and prevent relapse in MM.

Recent advancements in modern pharmacological studies have unveiled that traditional Chinese medicine (TCM) has a unique

"BCPT recognizes the potential of Natural Product studies in the identification of new therapies but wishes to emphasize that findings based on uncharacterized mixtures of compounds are preliminary in nature and serve primarily as hypothesis-generating to form the basis for more elaborate investigations." Mengjie Guo, Han Meng and Yi Sun have contributed equally to this work.

Summary

Bruceine A is a natural quassinoid derived from *Brucea javanica*, which is widely used for cancer treatment. However, the effectiveness and concrete mechanisms of Bruceine A for haematological malignancies, particularly for multiple myeloma (MM), remain unclear. In this study, we demonstrate that USP13, identified as a potential target of Bruceine A, stabilizes PARP1 protein through deubiquitination. Furthermore, Bruceine A targets the USP13/PARP1 signalling pathway to disrupt DNA damage repair in MM cells, inducing cell apoptosis and hampering MM progression in vitro and in vivo. These findings highlight the potential of Bruceine A as a promising strategy for the management of MM.

ability to target multiple pathways simultaneously, utilize various components and have multi-dimensional effects. This holistic approach enables it to inhibit tumour growth by comprehensively regulating the immune microenvironment [3]. As reported, over 60% of current anticancer medications are derived from natural sources [4]. One such natural source is *Brucea javanica* (L.) Merr (BJ) possesses strong anticancer properties against various types of cancers. BJ contains a variety of natural constituents, including tetracyclic triterpene quassinoids, sesquiterpenes, oleic acid, olein, linoleic acid, anthraquinone and pregnane glucoside [5]. The tetracyclic triterpene quassinoids, in particular, are known as the primary bioactive compounds in BJ that exert anticancer effects. One of these compounds, Bruceine A (BA), is derived from BJ and has a range of biological activities, such as inhibiting the growth of *Babesia gibsoni*, treating colon cancer and providing protective effects against diabetic nephropathy [6]. However, the potential effectiveness and specific mechanisms of BA as a treatment for MM are not well understood.

The active ingredients in TCM are essential for its therapeutic effects, as they work by interacting with specific biological targets. Identifying these targets is crucial for understanding the pharmacological mechanisms that underlie the efficacy of TCM [7]. Therefore, our research aimed to explore the mode of action and intrinsic targeted molecular pathways of BA in MM. We analysed proteome microarray data from a previous study and identified that Ub-specific protease 13 (USP13) was screened out as a potential target of BA [8]. Deubiquitinases (DUBs) are a class of enzymes that remove ubiquitin chains from target proteins, thereby stabilizing their expression [9, 10]. USP13, a critical member of the Ub-specific protease (USP) subfamily of DUBs, regulates the ubiquitination levels of various substrate proteins involved in cellular processes, such as cell cycle regulation, autophagy, metabolism, innate antiviral defence and DNA damage repair (DDR) [11]. Importantly, USP13 is associated with tumorigenesis from multiple perspectives, which remains controversial [12]. As documented, USP13 acts as an oncogene in the tumorigenesis of ovarian cancer by modulating cancer metabolism and promoting metastasis [13]. However, in other types of cancer such as oral squamous cell carcinoma, colorectal cancer and bladder cancer, USP13 functions as a tumour suppressor by maintaining the stability of PTEN [14–16]. Despite extensive research on the biochemical and molecular activities of USP13 in various human solid tumours, its role in haematological malignancies, particularly MM, has not been reported.

In this study, we investigated the role of USP13 in the development of MM both in vitro and in vivo. Additionally, we identified the mechanism by which USP13 affects the progression of MM. Furthermore, we examined the potential anticancer effects of BA by targeting USP13. Our research not only identifies USP13 as a potential target for MM treatment, but also provides new insights into the use of BA as a treatment for MM.

2 | Materials and Methods

The study was conducted in accordance with the Basic &Clinical Pharmacology & Toxicology Policy for Experimental and Clinical Studies [17]. The study was conducted in accordance with the Basic & Clinical Pharmacology & Toxicology policy for natural products [18].

2.1 | Database Analysis

RNA sequencing data for MM and normal tissues were obtained from The Cancer Genome Atlas (TCGA) and the Genotype-Tissue Expression (GTEx) database. The data were then analysed using the web tool available at http://gepia.cancer-pku.cn. Gene expression profiling (GEP) data were sourced from the GEO database, as previously described [19]. In addition, publicly accessible gene expression profile data from the Total Therapy 2 (TT2) cohort, Total Therapy 3 (TT3) cohort, and the Assessment of Proteasome Inhibition for Extending Remission (APEX) patient cohort (GSE5900) were included in our analyses. The patients were divided into groups based on disease progression or bone lesions, and the differences in USP13 expression were further examined using ANOVA or t-test. We utilized X-tile software to generate the Kaplan–Meier survival curve for patients and determined statistical significance using the Log-rank test.

2.2 | Antibodies and Reagents

The antibodies used in this study were as follows: USP13 (16 840-1-AP, ProteinTech Group, China); Flag (66008-3-lg, ProteinTech Group, China); β-actin (60008-I-Ig, ProteinTech Group, China); PARP1 (13371-1-AP, ProteinTech Group, China); Ubiquitin (10201-2-AP, ProteinTech Group, China); Goat anti-mouse IgG-HRP (ab150113, Abcam, UK); Goat anti-rabbit IgG-HRP (ab150077, Abcam, UK); BA was purchased from the Aladdin (Shanghai, China). Bortezomib (BTZ) was purchased from Selleck Chemicals (Houston, TX). APC Annexin V was purchased from BioLegend, Inc. (California, USA). Cell Counting Kit-8 (CCK-8) was purchased from Apexbio (Houston, USA).

2.2.1 | Cell Lines and Cell Culture

The human MM cell lines ARP1, KMS28PE, CAG, MM1S, 8226, JJN3, KMS11, H929, U266, LP-1 and KMS28BM were cultured

in RPMI1640. HEK293 cells were cultured in DMEM (Thermo Fisher Science, USA). The culture medium was supplemented with 10% foetal bovine serum (American Gibco), penicillin (100 U/mL, HyClone USA), and streptomycin (100 μg/mL, HyClone, USA) and was replaced every 2 days. All cells were cultured in 100 mm dishes at 37°C in a 5% CO_2 incubator.

2.2.2 | Plasmids and Cell Transfection

The plasmid containing the cDNA of human USP13 was supplied by TranSheepBio (Shanghai, China). The USP13 cDNA was inserted into the PTSB vector, which was equipped with GFP fluorescence and a Flag tag. The expression vector for USP13 cDNA and packaging vectors (pSPAX.2, pMD2.G) were simultaneously co-transfected into HEK293 cells using Lipofectamine transfection reagent (YEASEN, Shanghai). After 48 h, the viral supernatant was harvested, concentrated and stored at −80°C. The efficiency of lentiviral transfection in the cell lines was determined by puromycin selection.

BTXpress Cytoporation Media T4 (BTX, 47-0003) was used to deliver PARP1 siRNA into cells according to the Manufacturer's manual. A suspension containing 5×10^5 MM cells was prepared in 500 μL of BTXpress Cytoporation Media T4 (47-0003, BTX), followed by the addition of siRNA to achieve a final concentration of 100 nmol/L. The mixture was then transferred to an electroporation cuvette for thorough mixing and subsequent transfection. Sequences of PARP1 siRNA were as following:

negative control, sense 5′-UUCUCCGAACGUGUCACGUTT-3′ and anti-sense 5′-ACGUGACACGUUCGGAGAATT-3′;

PARP1-si1, sense 5′-CGCCCAUGUUUGAUGGAAATT-3′ and anti-sense 5′-UUUCCAUCAAACAUGGGCGTT-3′;

PARP1-si2, sense 5′-GGUGAUCGGUAGCAACAAATT-3′ and anti-sense 5′-UUUGUUGCUACCGAUCACCTT-3′;

PARP1-si3, sense 5′-GCCAAGUCCAACAGAAGUATT-3′ and anti-sense 5′-UACUUCUGUUGGACUUGGCTT-3′;

PARP1-si4, sense 5′-GACCUCAUCAAGAUGAUCUTT-3′ and anti-sense 5′-AGAUCAUCUUGAUGAGGUCTT-3′.

2.3 | Cell Proliferation and Colony Formation

In the CCK-8 assay, 1.5×10^3 MM cells were plated in each well of a 96-well format. Subsequently, CCK-8 solution was added to each well and the cells were incubated for 24, 48 and 72 h. The optical density was then determined at a wavelength of 450 nm utilizing a microplate reader (Varioskan LUX, Thermo). Colony formation assay was performed to assess the proliferation and clonogenic growth ability of MM cells. MM cells were cultured at a density of 1×10^4 per well in a 24-well plate with 0.5 mL of a mixture containing 0.33% agar in RPMI 1640 medium enriched with 10% FBS. The culture medium was replenished biweekly for a duration of two weeks. Finally, the colonies were visualized and counted.

2.4 | Co-Immunoprecipitations (Co-IP) and Western Blotting (WB)

WB was conducted according to previous protocols [19]. Following the guidelines provided by the manufacturer, the Pierce Direct Magnetic IP/CO-Immunoprecipitation (Co-IP) Kit (Thermo Scientific) was utilized to carry out the Co-IP analysis.

2.5 | Mass Spectrometry (MS) Analysis

SDS-PAGE was utilized to separate proteins, followed by the excision and enzymatic digestion of gel bands using sequencing-grade trypsin (Promega, USA). The resulting peptides were then analysed with a Qexactive mass spectrometer (Thermo Fisher Scientific). The fragment spectra were subsequently queried against the National Center for Biotechnology Information's Non-Redundant Protein Database. The original contributions presented in the study are publicly available and can be accessed through the Proteome Xchange Consortium at PXD057487. The dataset can be accessed by logging in to the PRIDE website using the following details: Project accession: PXD057487; Token: Kqbcsdljy7D3.

2.6 | MM Cell Line-Derived Xenograft (CDX) Model

We administered a subcutaneous injection of 1×10^6 pCDH-EV (EV) and USP13-OE MM cells into the left and right abdominal regions of 6- to 8-week-old NOD/SCID mice ($n = 6$ per group), respectively. Tumour diameters were measured thrice weekly using callipers. Upon reaching a tumour size of 15 mm, the mice were euthanized via intraperitoneal injection of pentobarbital sodium anaesthesia. Subsequently, the tumours were harvested, weighed and photographed.

2.7 | MM Patient-Derived Tumour Xenograft (PDX) Model

The biopsy sample was taken from tumour tissue excised from patients with MM at Nanjing Hospital of Chinese Medicine affiliated with Nanjing University of Chinese Medicine. The tissue was excised into cubes measuring $2.5 \times 2.5 \times 2.5\ mm^3$ and then transplanted subcutaneously into 6- to 8-week-old NOD/SCID mice (five mice per group), using 1% sodium pentobarbital for anaesthesia. After the tumours grew to a volume of $500\ mm^3$, they were cut into $2.5 \times 2.5 \times 2.5\ mm^3$ pieces and re-implanted into the mice. This cycle was repeated three times to ensure consistent tumour development. Once the tumour diameter reached 5 mm, the mice were randomly assigned to three groups: a control group, a group treated with BTZ (BTZ, 1 mg/kg, i.p.), and a group treated with BA (BA, 4 mg/kg, i.p.). Treatments were administered twice a week. Once the tumour diameter reached 15 mm, the mice were sacrificed and tumour tissues were collected, weighed and photographed.

2.8 | 5TMM3VT Mouse Model

A sufficient number of 5TMM3VT cells were amplified during the logarithmic growth phase. Subsequently, the cells were centrifuged at 1200 rpm for 5 min at room temperature. The supernatant was discarded, and the cell pellet was washed twice with PBS. Then, the cell density was adjusted to 1×10^7/mL using PBS. A total of 100 μL of the 5TMM3VT cell suspension was injected into C57BL/KaLwRij mice obtained from Harlan Laboratories via the tail vein. The mice were then randomly divided into two groups: a control group and a BA treatment group, each consisting of 10 mice. On the third day following cell injection for modelling purposes, the treatment group received intraperitoneal injections of BA at a dosage of 4 mg/kg twice weekly, while the control group received physiological saline via intraperitoneal injections. The mice would be sacrificed, once they exhibited signs of hindlimb weakness.

All relevant animal experiments were conducted with the approval of the Animal Ethics Committee of Nanjing University of Chinese Medicine (202207A076).

2.9 | Statistical Analysis

Data were displayed as the mean ± standard deviation. A two-tailed Student's *t*-test was utilized to compare two groups, while one-way ANOVA was employed to assess differences among multiple groups. The Kaplan–Meier method, in conjunction with the Log-rank test, was used to evaluate the survival rates of patients with MM. Specific *p*-values for all comparisons were included in the statistical charts.

3 | Results

3.1 | USP13 is Identified as a Potential Target of BA in MM

In order to identify potential therapeutic targets for BA in MM, our research group analysed proteome microarray data from studies conducted by Zhao et al. This analysis revealed a strong interaction between USP13 and BA (Figure 1A). To further validate this finding, we used microscopic thermophoresis (MST) to confirm the binding of BA to the human recombinant USP13 protein, as depicted in Figure 1B. We then investigated whether dysregulation of USP13 expression was associated with MM development. GEPIA database showed that USP13 was abnormally upregulated in various types of cancers (Figure 1C). Additionally, we examined the GEP of USP13 in normal plasma (NP) cells, monoclonal gammopathy of undetermined significance (MGUS) and MM bone marrow plasma cells. Our analysis revealed a significant increase in USP13 expression in patient with MM plasma cells compared to NP ($p < 0.05$) and MGUS cells ($p < 0.01$), but no significant difference between NP and MGUS cells. These findings suggest that USP13 dysregulation occurs during the transition from MGUS to MM (Figure 1D). Furthermore, we explored the role of USP13 in the prognosis of patients with MM using Kaplan–Meier survival analysis. The data demonstrated that patients with MM with high USP13 expression had worse overall survival (OS) compared to those patients with low USP13 expression in TT3 ($p < 0.05$) and APEX ($p < 0.0001$) patient cohorts, respectively (Figure 1E,F). Overall, these results confirmed that USP13 may serve as a potential target for BA and potentially have diagnostic and prognostic implications in MM.

3.2 | Overexpression of USP13 Promotes MM Cell Proliferation

To assess the role of USP13 in MM, we first conducted a WB experiment to detect the endogenous expression level of USP13 in commonly used MM cell lines. The results showed that USP13 protein was expressed in all MM cell lines examined, with moderate levels in the ARP1 and KMS28PE cell lines (Figure 2A). Therefore, we chose ARP1 and KMS28PE cell lines as in vitro experimental models for MM. Next, we used a lentivirus-based method to establish stable overexpression (OE) of USP13 in ARP1 and KMS28PE MM cell lines, which was confirmed by WB analysis (Figure 2B). The viability of empty vector (EV) and USP13-OE MM cells was assessed using the CCK-8 assay at 24, 48 and 72 h post-transfection. The USP13-OE cells exhibited a markedly higher cell growth rate than the EV cells (Figure 2C). Furthermore, the effect of USP13 overexpression on the long-term proliferation of MM cells was validated via clonogenic soft agar assay. Compared to the EV group, USP13 overexpression significantly enhanced the long-term proliferation ability of MM cells (Figure 2D). To extend these findings in vivo, we subcutaneously injected 1×10^6 ARP1 EV cells (left flank) and ARP1 USP13-OE cells (right flank) into NOD/SCID mice. As shown in Figure 2E,F, we visually observed that tumours generated in the USP13-OE group grew faster than those in the EV group. Additionally, the mean weight (Figure 2G) and volume (Figure 2H) of the tumours were also significantly higher in the USP13-OE group. WB analysis also showed a significant increase in USP13 expression in the tumours of the USP13-OE group compared to the EV group (Figure 2I). These findings suggest that USP13 functions as an oncogene to promote the proliferation of MM cells.

3.3 | PARP1 is Identified as a Downstream Target of USP13 in MM

The above studies have confirmed that USP13 plays an oncogenic role in MM. In order to clarify the mechanism by which USP13 promotes MM proliferation, we planned to conduct MS analysis on ARP1 WT and USP13-OE cells. The results of Gene Ontology (GO) and KEGG pathway analysis on the MS data indicated that the mechanism of action of USP13 in MM was closely linked to DDR related signalling pathways (Figure 3A,B). The intersection of all up-regulated 580 genes in the two pairs of cells was shown in the Venn diagrams (Figure 3C). We searched for the downstream target genes positively associated with DDR and the progression of MM. Additionally, a previous study has shown that USP15 can interact with PARP1 [20]. Based on this strategy, we identified PARP1 as a downstream target of USP13 in MM. The presence of PARP1-specific peptide segments was confirmed by MS analysis (Figure 3D). PARP1 was found to be significantly increased in patients with newly diagnosed MM ($n = 351$)

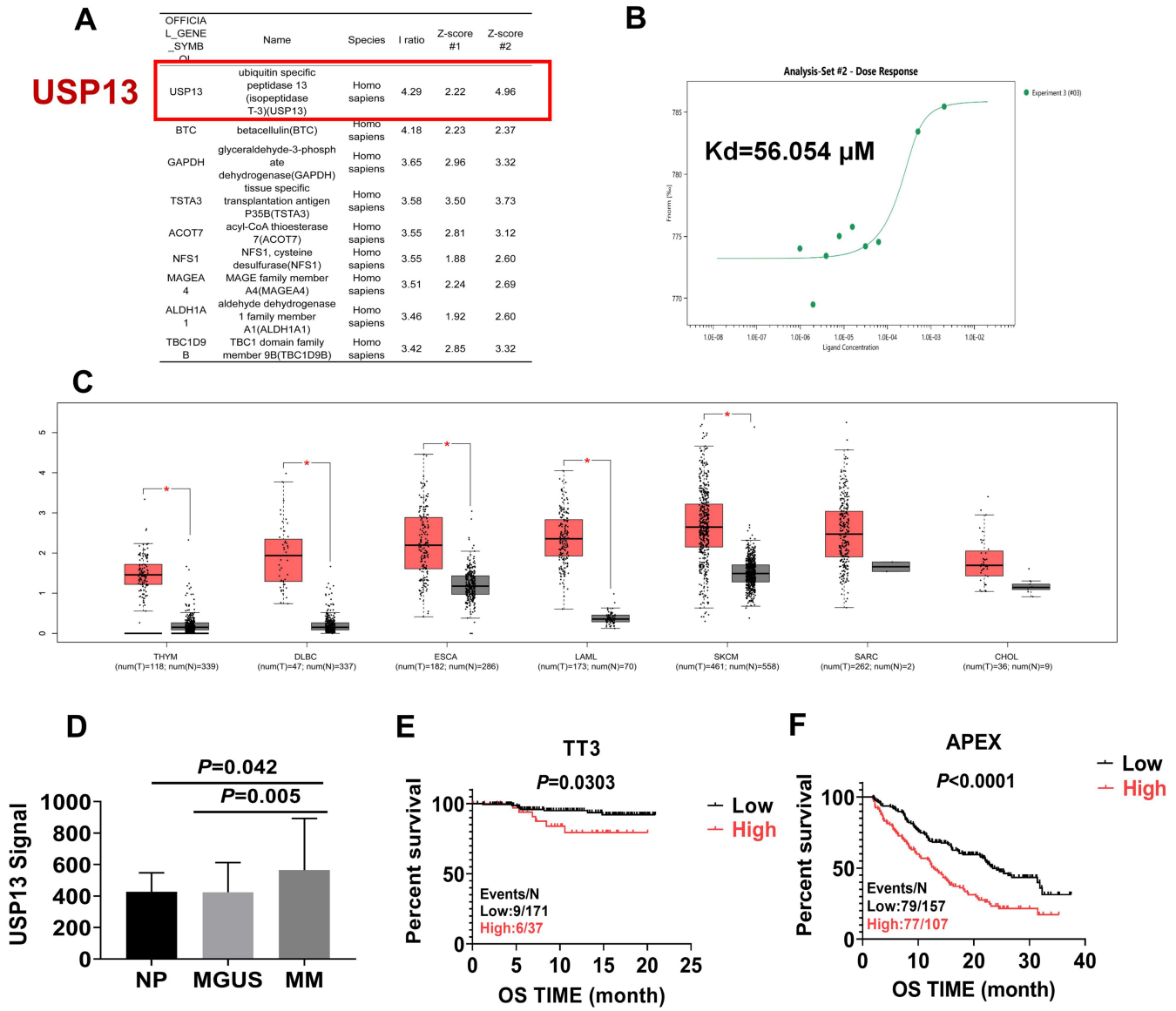

FIGURE 1 | USP13 is identified as a potential target of BA in MM. (A) Analysis of proteome microarray data from a previous study identified USP13 as a potential target of BA [8]. (B) MST technology confirmed that USP13 protein has a strong binding affinity to BA. (C) The TCGA database showed a significant increase in USP13 gene expression in various tumour tissues compared to normal tissues. (D) USP13 mRNA levels were notably elevated in MM samples, with the y-axis representing the signal level of USP13. Patients were divided into three groups: healthy donors with normal bone marrow plasma cells (NP, $n = 22$), monoclonal gammopathy of undetermined significance (MGUS, $n = 44$), or multiple myeloma (MM, $n = 351$), and they were sorted on the x-axis. (E & F) Upregulated USP13 mRNA expression was correlated with poor overall survival (OS) in MM patients from the TT3 (E) and APEX (F) patient cohorts. The data are expressed as mean ± SD.

compared to patients with MGUS ($n = 44$) and healthy individuals ($n = 22$) ($p < 0.001$) (Figure 3E). Furthermore, patients with MM with high PARP1 expression exhibited shorter OS in the TT2 ($p < 0.0001$) (Figure 3F) and APEX ($p < 0.0001$) (Figure 3G) cohorts. Then, Co-IP and reverse Co-IP experiments further determined the physiological interaction between USP13 and PARP1 (Figure 3H,I).

3.4 | USP13 Stabilizes PARP1 Protein Through Deubiquitination in MM

To clarify the interaction between USP13 and PARP1, we conducted a WB examination. The results showed that overexpression of USP13 increased the protein expression of PARP1 in ARP1 (Figure 4A) and KMS28PE (Figure 4B) cell lines. To further investigate the relationship between USP13 expression and PARP1 protein stability, we measured the levels of PARP1 at different time points after adding 50 μg/mL of cycloheximide (CHX) to ARP1/KMS28PE EV and USP13-OE cells. As a result, we found that the half-life of PARP1 protein was significantly prolonged in USP13-OE cells compared to EV cells (Figure 4C,D), indicating that USP13 positively affects PARP1 protein stability. Previous studies have shown that USP13 plays a role in the occurrence and development of various cancers by deubiquitinating diverse substrates [10]. Therefore, we aimed to determine if USP13 can regulate PARP1 expression through deubiquitination. Further ubiquitination experiments, after

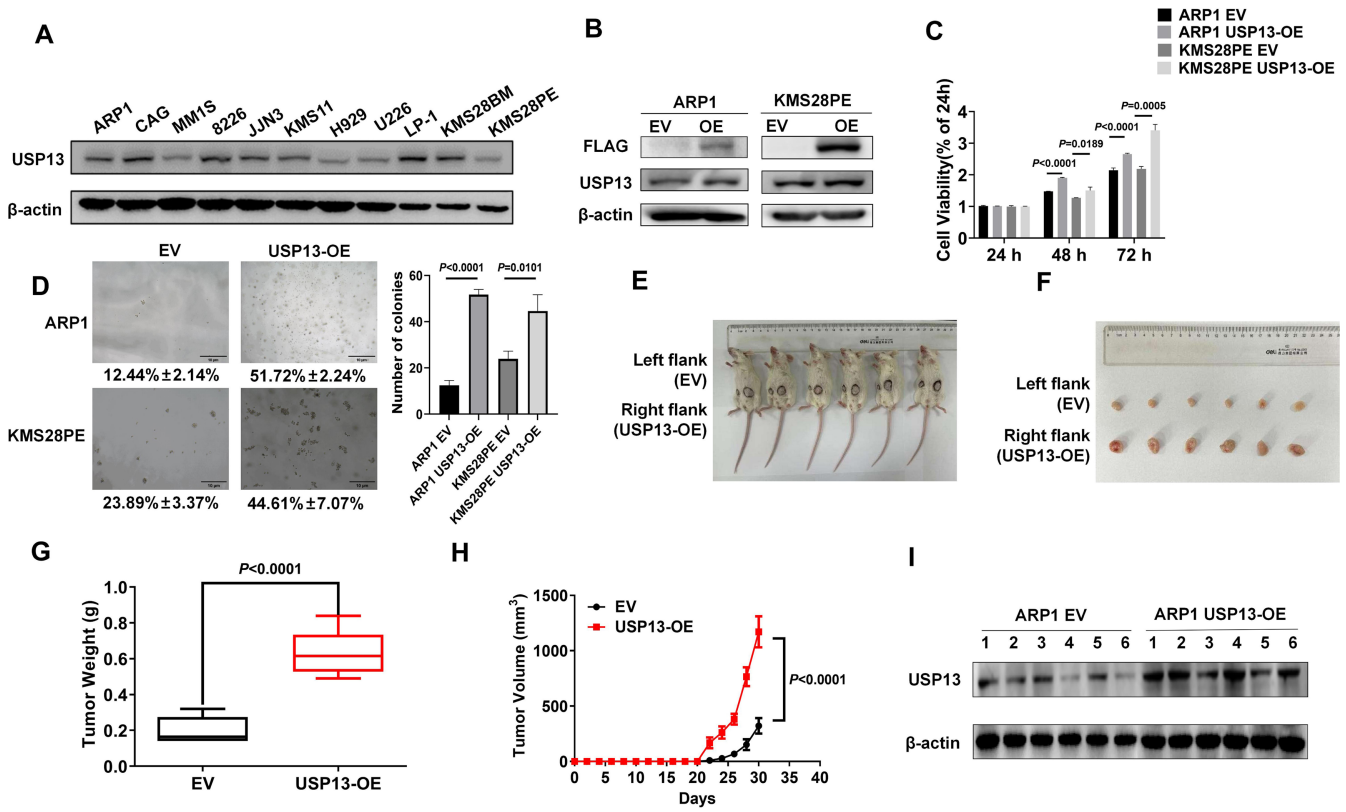

FIGURE 2 | Overexpression of USP13 promotes MM cell proliferation. (A) WB analysis confirmed the endogenous expression of USP13 in the specified MM cell lines. (B) The increased expression of USP13 was verified in USP13-OE ARP1 and KMS28PE cell lines compared to vehicle-transfected control cells. (C) CCK-8 assay showed that overexpression of USP13 promoted the growth of MM cells ($n = 3$). (D) Soft agar cloning experiment determined that induction of USP13 enhanced the long-term proliferation of MM cell lines ($n = 3$). (E) Photographic images of mice injected with MM cells transfected with EV and USP13-OE plasmid in each flank ($n = 6$). (F) Photographs of harvested xenograft tumours. (G & H) The time course of tumour weight (G) and mean tumour volume (H) from two experimental groups. (I) WB detection of USP13 expression level in tumour tissues. The data are expressed as the mean ± SD.

treatment with 20 μM MG132, demonstrated that increased expression of USP13 can enhance the deubiquitination of PARP1 protein, leading to reduced degradation (Figure 4E,F). These results suggest that PARP1 is a potential substrate of USP13, which can be directly deubiquitinated by USP13 to promote its protein stability in MM.

3.5 | USP13/PARP1 Axis Positively Regulates MM Cell Proliferation by Activating DDR

To investigate the role of PARP1 in MM malignancy in vitro, we utilized siRNA to knocked down PARP1. The effectiveness of the knockdown was confirmed through WB analysis, with si-2 showing the strongest interference (Figure 5A,B). CCK-8 assay showed a significant decrease in cell growth rate in ARP1 and KMS28PE cells over time after PARP1 silencing (Figure 5C), confirming that PARP1 facilitated MM cell proliferation. Then, we investigated the mechanism behind the USP13/PARP1-mediated promotion of MM progression. Previous studies have shown that PARP1's catalytic activity plays a crucial role in regulating various DDR pathways [21]. Therefore, we hypothesized that USP13/PARP1 may enhance MM cell proliferation by mediating DDR. To assess the impact of USP13/PARP1 on MM cell DDR, we performed the comet assay, a versatile method for detecting nuclear DNA damage [20]. Meanwhile, we treated MM cells with the chemical methylating agent methyl methane sulfonate (MMS), a highly toxic DNA-alkylating agent inducing DNA damage. As shown in Figure 5D, treatment with MMS significantly exacerbated the DNA damage in MM cells. However, overexpression of USP13 reduced the degree of DNA damage, effectively reversing the DNA damage caused by MMS treatment to the same level as the control group. In addition, knocking down PARP1 triggered the DNA damage in MM cells, while upregulation of USP13 can alleviated the DNA damage induced by interfering with PARP1 (Figure 5E). These findings confirm that the USP13/PARP1 axis positively regulates the DDR of MM cells, promoting MM cell proliferation.

3.6 | BA Inhibits MM Cell Proliferation in Vitro by Targeting the USP13/PARP1 Axis

After identifying oncogenic USP13 as a potential therapeutic target for BA and understanding how it contributes to MM progression, we conducted further research to determine if BA could inhibit MM cell proliferation induced by USP13. To assess the impact of BA on USP13 protein levels in MM cells, we performed WB analysis on both EV and USP13-OE MM cells treated with 0.2 μM BA. The results showed that BA significantly

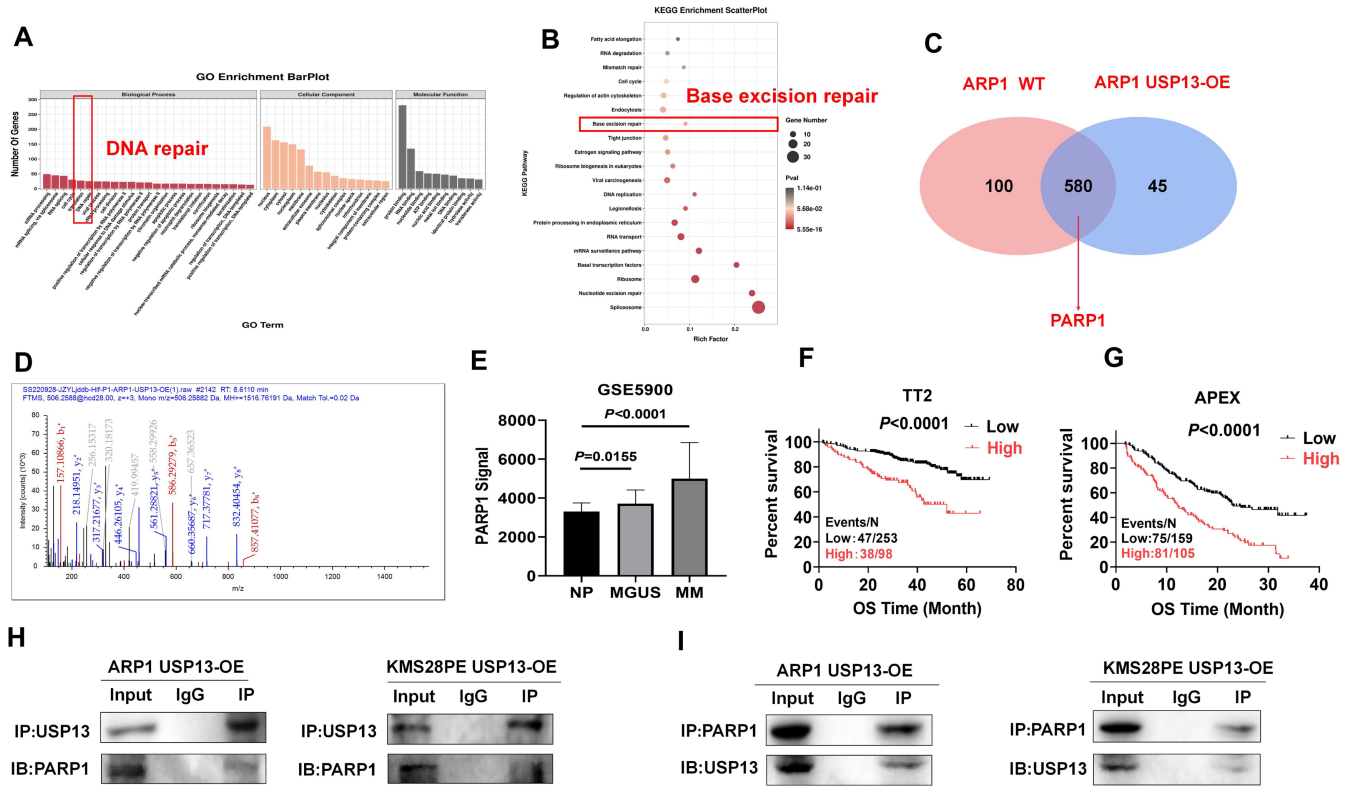

FIGURE 3 | PARP1 is identified as a downstream target of USP13 in MM. (A) Gene ontology (GO) analysis was conducted on ARP1 WT/USP13-OE cell lines using MS analysis. (B) Kyoto Encyclopedia of Genes Genomes (KEGG) pathway classification was also performed on ARP1 WT/OE cell lines via MS analysis. (C) USP13 was identified through a Venn diagram analysis of the upregulated genes in two groups. (D) MS analysis identified specific peptides from PARP1. (E) USP13 mRNA levels were significantly elevated in MM samples. The y-axis shows the signal level of USP13, and the x-axis shows the three groups of patients: healthy donors with normal bone marrow plasma cells (NP, $n=22$), monoclonal gammopathy of undetermined significance (MGUS, $n=44$), or multiple myeloma (MM, $n=351$). (F & G) Increased PARP1 mRNA expression was correlated with poor overall survival (OS) in MM patients from the TT2 (F) and APEX (G) patient cohorts. (H & I) Co-IP assays showed that USP13 interacted with PARP1 in both MM cell lines, as demonstrated by forward (H) and reverse (I) experiments. The data are expressed as mean ± SD.

reduced the protein expression of USP13 (Figure 6A). Moreover, PARP1, a potential target of USP13, was also inhibited by BA treatment in both EV and USP13-OE MM cells (Figure 6B), indicating that BA can interfere with USP13/PARP1 axis. We then tested the IC_{50} of BA for MM treatment using MTT assay. The data revealed that BA inhibited MM cell proliferation in a dose-dependent manner, and overexpression of USP13 led to resistance to BA treatment (EV: 0.3379 μM vs. USP13-OE: 10.56 μM, Figure 6C). PARP and Caspase-3 are two crucial molecules involved in the process of apoptosis in various types of cancer. Our Western blot analysis revealed an increase in cleaved PARP and cleaved Caspase-3 levels, as well as a decrease in USP13 expression in BA-treated cells compared to untreated cells (Figure 6D). Then, flow cytometry experiment was adopted to detect the effect of BA on the apoptosis of MM cells. The results showed that BA significantly induced apoptosis in both EV and USP13-OE MM cells (Figure 6E). In order to overcome the resistance to BA induced by USP13 overexpression, we combined BA with the PARP inhibitor olaparib. CCK-8 assay and flow cytometry analyses demonstrated that the combination of BA and olaparib effectively inhibited cell proliferation and enhanced cell apoptosis in USP13-OE MM cells compared to cells treatment with BA alone (Figure 6F,G). These findings suggest that combining BA with a PARP inhibitor can effectively counteract the resistance to BA induced by USP13 overexpression.

3.7 | BA Hampers MM Progression in Mouse Models

To further validate the effect of BA in inhibiting USP13 in vivo and evaluate its effectiveness in treating MM at a clinical level, we administered BA to PDX mice. Tumours were harvested from the subcutaneous tissue of patients with MM and subsequently inoculated them into NOD/SCID mice. The mice were then treated with both BTZ and BA, and the growth of xenograft tumours was monitored (Figure 7A). Once the tumour diameter reached 15 mm, the mice were sacrificed and the tumour tissues were collected, weighed, and photographed. As shown in Figure 7B,C, the tumours in the BA-treated group were significantly smaller than those in the control group. Consistently, the mean volume and weight of tumours in the BA-treated group were significantly lower than those in the control group (Figure 7D,E). In addition, we found that the anticancer effect of BA on MM was comparable to that of BTZ. We also utilized the 5TMM3VT mouse model to evaluate the pharmacological effect of BA on MM progression. 5TMM3VT cells were injected into the tail veins of C57BL/KaLwRij mice, which mimicked the MM bone marrow microenvironment in vivo [22] (Figure 7F). The mice were sacrificed once they exhibited signs of hind-limb weakness. The data showed that BA greatly extended the survival of 5TMM3VT mice compared to the control group

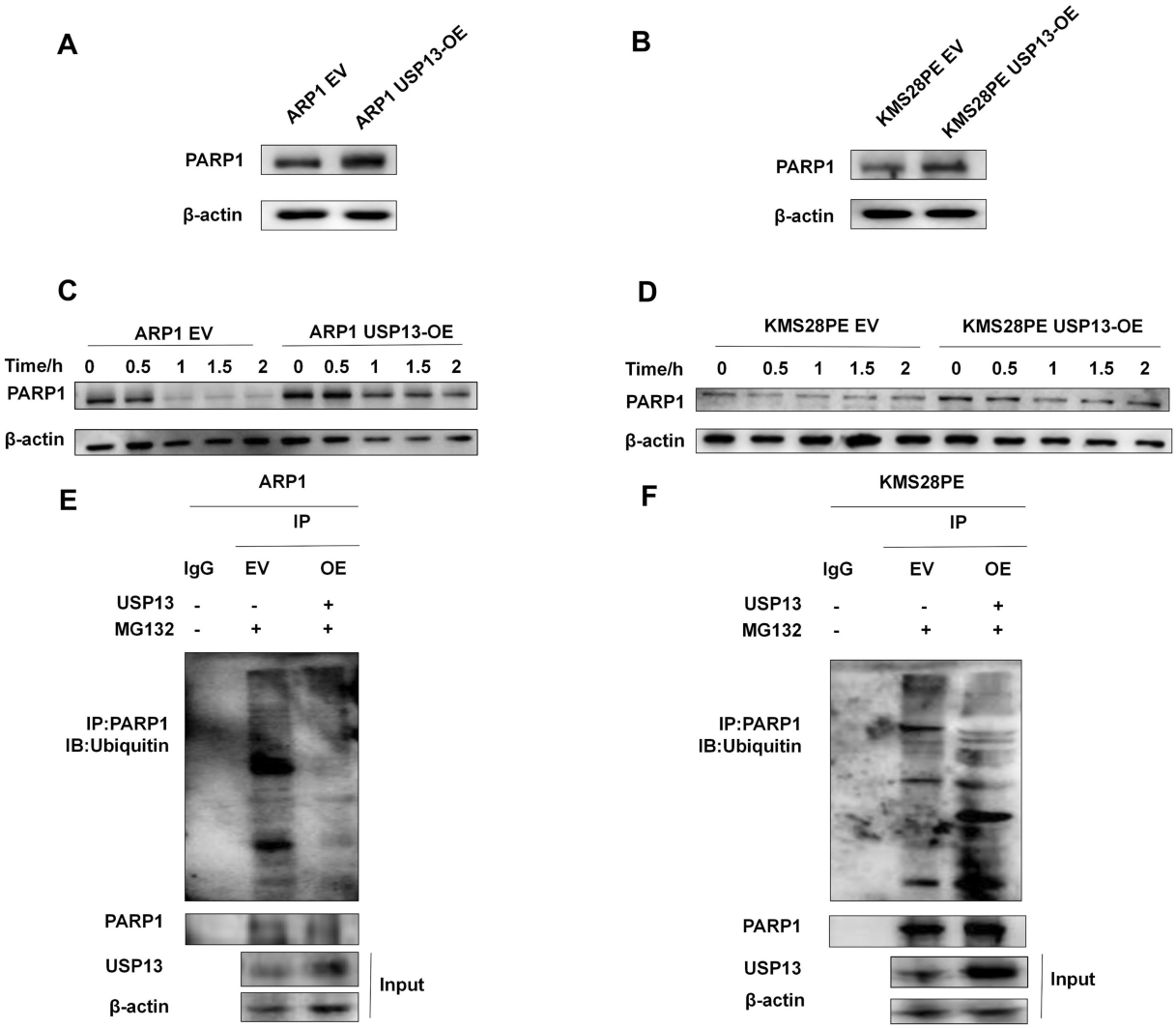

FIGURE 4 | USP13 stabilizes PARP1 protein through deubiquitination in MM. (A & B) WB analysis revealed that increased levels of USP13 resulted in higher protein expression of PARP1 in ARP1 (A) and KMS28PE (B) cell lines. (C & D) Detection of the effect of USP13 overexpression on the half-life of PARP1 protein expression after adding CHX in ARP1 (C) and KMS28PE (D) cell lines. (E & F) Co-IP experiments were performed after treatment with 20 μM MG132 to assess the effect of increased USP13 expression on the ubiquitination of PARP1 in ARP1 (E) and KMS28PE (F) cell lines.

(Figure 7G). These findings demonstrate that BA can retard the development of MM by targeting USP13/PARP1-mediated DDR and triggering cell apoptosis, providing a novel mechanism of action for BA in MM (Figure 7H).

4 | Discussion

The activities of deubiquitinating enzymes (DUBs) in cancer are well-established, as they play a crucial role in stabilizing the proteins that regulate disease progression [23]. Increasing evidence suggests that DUBs also play a significant role in the development of haematological malignancies, particularly in pathways related to cellular energy metabolism, continuous cell division, and genetic instability [24, 25]. Furthermore, specific DUBs are crucial for the differentiation of haematopoietic stem cells (HSCs) into various blood cell lineages, and disruptions in this process are linked to haematological malignancies [26–28]. Recent studies on the role of deubiquitinating enzymes in the development of MM have revealed the potential for targeting these enzymes as a therapeutic approach [29]. The ubiquitin-specific proteases (USPs), a prominent family within the DUBs, consist of 58 members. USP1, which is involved in DDR and cell differentiation, is overexpressed in some cases of MM and is associated with a poor outcome [30]. USP5 can enhance the stability of c-Maf, promoting the growth and survival of MM cells [31]. Overexpression of USP7 is linked to a poor prognosis, and inhibiting USP7 can effectively overcome resistance to BTZ in MM [32]. While USP13 shares approximately 80% sequence similarity with USP5 [33], there is limited research on its role in MM. In this study, we utilized data from patients with MM, cell lines, and three mouse models to confirm that USP13 plays a significant role in the malignant development of MM and could serve as a potential therapeutic target.

USP13 plays a significant role in the development of cancer by removing ubiquitin from proteins that can either promote or inhibit tumour growth [10]. However, due to the complexity and

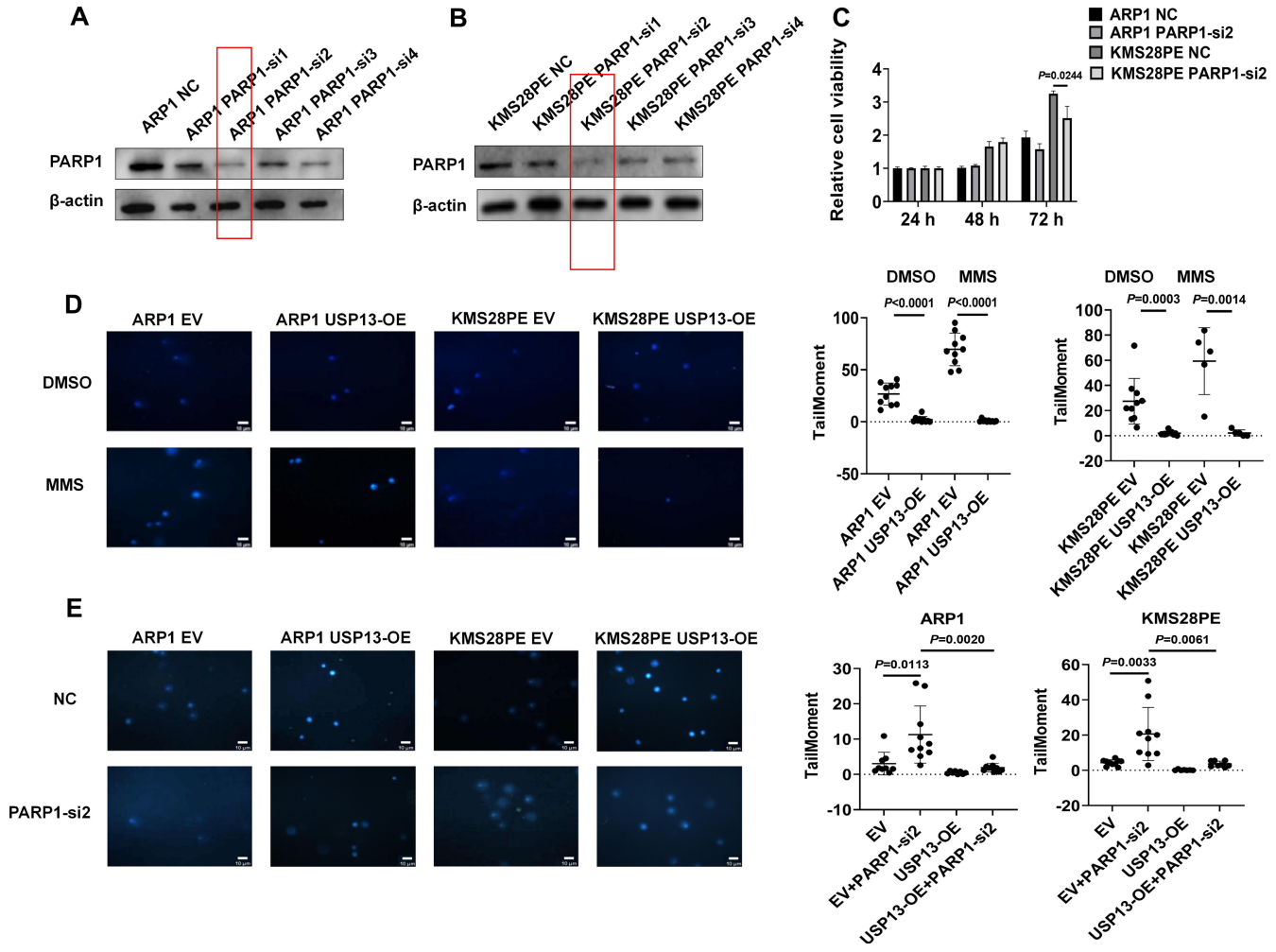

FIGURE 5 | USP13/PARP1 axis positively regulates MM cell proliferation by activating DDR. (A & B) The expression of PARP1 was validated through WB analysis after treatment with different siRNAs, and it was found that si-2 had the most effective interference. (C) Inhibition of PARP1 expression significantly suppressed MM cell proliferation ($n = 3$). (D) Comet assay results showed that overexpression of USP13 greatly reduced the DNA damage caused by MMS treatment ($n = 10$). (E) Comet assay results also demonstrated that interference with PARP1 led to DNA damage in MM cell lines, while upregulation of USP13 activated DDR and reduced DNA damage by inhibiting PARP1 ($n = 10$). The data are expressed as mean ± SD.

diversity of the proteins involved, it is difficult to definitively determine the specific role of USP13 in regulating cell cycle, DDR, endoplasmic reticulum-associated degradation (ERAD), and autophagy [34]. Interestingly, our study discovered that USP13 plays a crucial role in stabilizing the PARP1 protein through deubiquitination. PARP1 is a member of the ADP-ribosyltransferase diphtheria toxin-like (ARTD)/PARP family, which is the most extensively studied enzyme [35]. PARP1 post-translationally attaches a negatively charged polymer called poly (ADP-ribose) (PAR) to itself and other target proteins [21]. This poly (ADP)ribosylation (PARylation) activity is implicated in various functions attributed to PARP1 within the DDR, particularly in repairing single-strand breaks (SSBs) and double-strand breaks (DSBs) [21]. Previous studies have demonstrated that pathways involved in the repair of DNA SSBs and DSBs are dysregulated in MM, which correlates with aggressive disease progression and a reduced response to autologous stem cell transplantation (ASCT) [36, 37]. Notably, inhibiting PARP1 through suppression or pharmacological intervention with olaparib has induced DNA damage in MM [37]. Our study also found that inhibiting PARP1 can effectively hinder DDR and impede MM cell proliferation, which can be reversed by interacting with USP13 to weaken its ubiquitination degradation. As reported, USP13 can precisely modulate multiple crucial proteins involved in DDR by deubiquitinating them, such as RAP80 and TopBP1, thereby targeting the DDR system [34, 38]. Consequently, efficient DSB repair is maintained, creating a safer microenvironment for the proliferation of cancer cells [34]. Our study reveals a new regulatory mechanism by which the USP13-PARP1 complex can be activated to promote MM progression by enhancing DDR, contributing to a comprehensive understanding of the regulatory spectrum governed by USP13.

There has been a growing interest in bioactive compounds derived from Traditional Chinese Medicine Materials (TCMMs), and their potential to combat MM has been extensively studied [39]. The diverse pharmacological effects of natural products can be achieved by targeting multiple pathways, thereby addressing cancer heterogeneity and mitigating drug resistance associated with conventional chemotherapy strategies [40]. Substances such as curcumin, resveratrol, baicalein, berberine, triterpene, bufadienolides, gambogic acid, ginsenoside

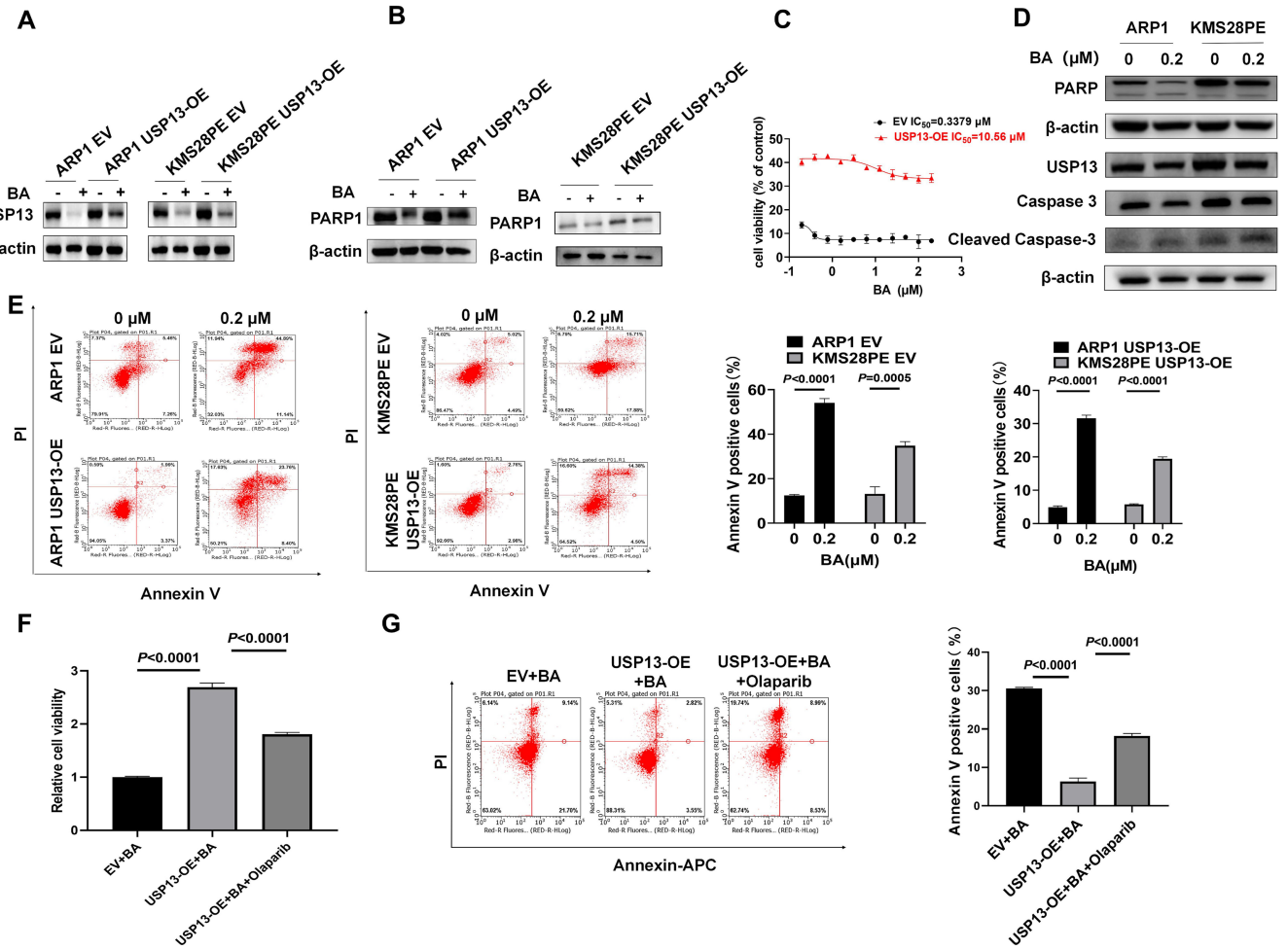

FIGURE 6 | BA inhibits MM cell proliferation in vitro via targeting USP13/PARP1 axis. (A) WB experiment detected the effect of BA on USP13 protein expression in EV and USP13-OE MM cells. (B) WB experiment detected the effect of BA on PARP1 protein expression in EV and USP13-OE MM cells. (C) The viability of MM cells, with or without overexpression of USP13, was measured after treatment with BA ($n = 3$). (D) WB analysis further confirmed that BA increased the expression of apoptotic proteins. (E) Flow cytometry analysis indicated that BA induced MM cell apoptosis ($n = 3$). (F) The effect of BA on cell proliferation was evaluated in USP13-OE cells, with and without olaparib. (G) Similarly, the effect of BA on cell apoptosis was also assessed in USP13-OE cells, with and without olaparib. The data are expressed as mean ± SD.

and other less-explored components have considerable anti-MM properties by inhibiting angiogenesis and cell growth [39]. In particular, numerous studies have identified triterpene compounds, such as KBB-N2, Asiatic acid, and DCZ0415, as targeted agents for MM treatment [41, 42], although the underlying mechanisms require further elucidation. BA is a naturally occurring tetracyclic triterpene quassinoid recognized for its potent anticancer properties and high safety and biocompatibility. Bruceine B shares a similar chemical structure with BA and demonstrates considerable anti-MM activity [43]. Inspired by these findings, we referenced a prior study that employed the bioactive anticancer molecule BA as a probe to demonstrate that USP13 exhibits a strong binding affinity towards BA. We subsequently confirmed that BA can hamper MM progression by targeting USP13/PARP1 and inducing cell apoptosis. Additionally, our findings show that combining BA with a PARP inhibitor, olaparib, can effectively counteract the resistance to BA induced by USP13 overexpression. Consistent with our observations, previous studies by Valdez BC et al. have shown that the PARP inhibitor olaparib enhances the cytotoxicity of gemcitabine, busulfan and melphalan in lymphoma cells [44]. Our research contributes to a better understanding of clinical effectiveness of using BA in combination therapy alongside PARP inhibitors.

Most studies on bioactive components have primarily focused on MM cells; however, it is still unclear whether these bioactive components possess cytotoxic effects [39]. In the present study, we also evaluated the pharmacological action of BA on MM in vivo using a PDX model and 5TMM3VT mouse model, demonstrating the significant effectiveness and minimal side effects of BA on mice. However, it is important to note that more comprehensive drug safety evaluation tests are necessary before BA can be clinically translated. Recently, researchers have been actively investigating the mechanisms by which BA suppresses tumour growth. For instance, Huang et al. discovered that BA exerted inhibitory effects on pancreatic cancer by targeting p38α [45]. Another study highlighted the role of BA in preventing colon cancer cell migration through its interaction with Bax [46]. Additionally, BA has been shown to inhibit breast cancer metastasis via modulation of the PI3K-AKT signalling pathways [46]. In summary, it has been documented that BA exerts anti-tumour

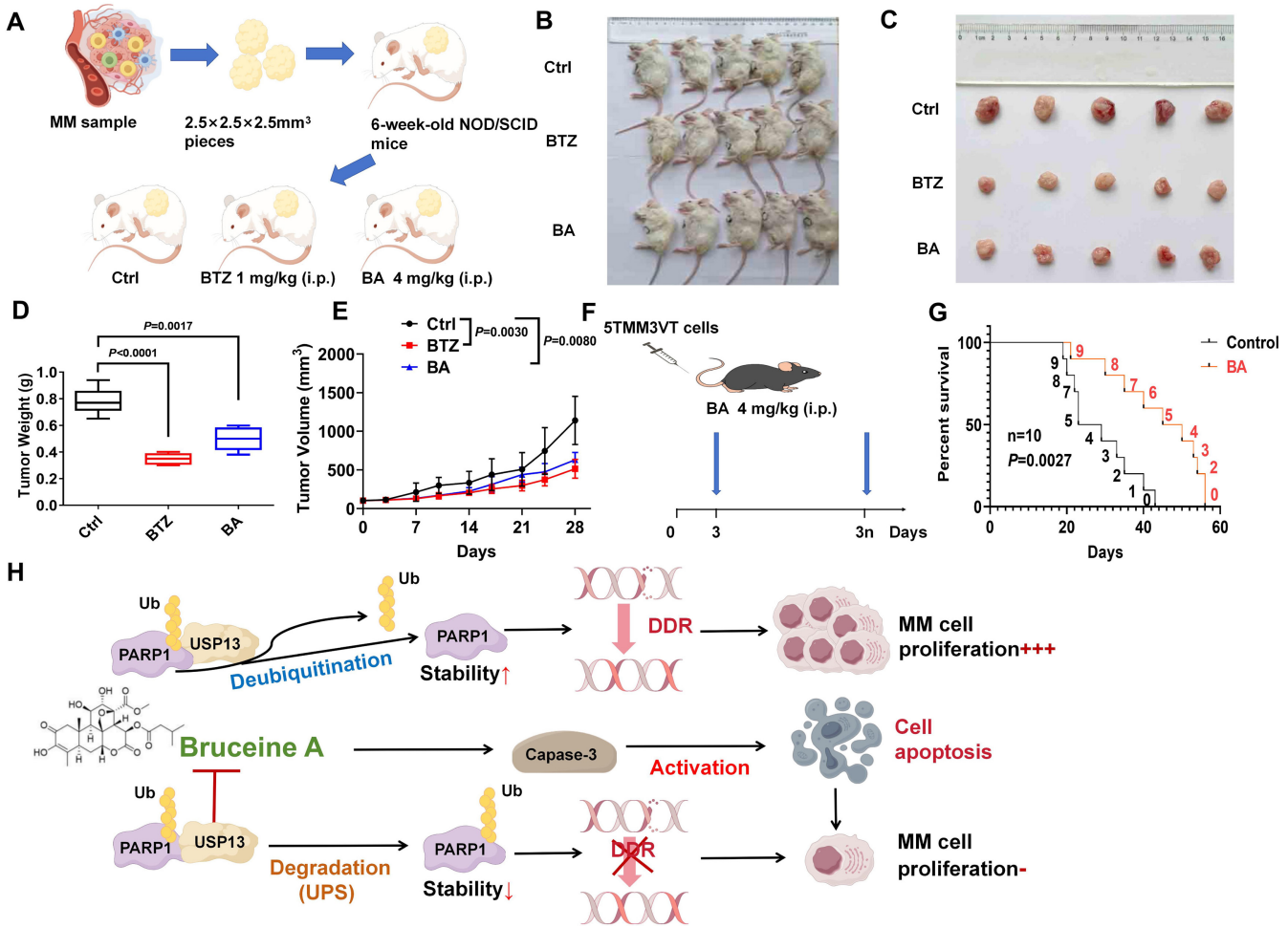

FIGURE 7 | BA hampers MM progression in mouse models. (A) Schematic representation of PDX mouse model. (B) Photographs of mice with xenografts ($n = 5$). (C) Images of tumours. (D) Tumour weight of PDX model mice in the ctrl, BTZ, and BA groups. (E) Time course of tumour volume in NOD/SCID mice after treatment with BTZ or BA. (F) Schematic representation of 5TMM3VT mouse model. (G) Treatment with BA significantly improved the survival time of 5TMM3VT mice ($n = 10$). (H) Schematic depiction illustrates that BA targets USP13/PARP1 axis to disrupt the DDR of MM cells and induce cell apoptosis to hamper MM progression.

effects through various mechanisms, such as apoptosis, autophagy, and oxidative stress in solid tumours. However, there is currently a lack of research exploring the mechanism of action of BA in haematological malignancies. The compound BA has shown the potential to inhibit tumour growth and metastasis through various pathways and mechanisms that may vary depending on the specific type of cancer. Our study provides novel insights into the anticancer effects of BA on MM, as it appears to disrupt DDR in MM cells by targeting the USP13/PARP1 axis and inducing cellular apoptosis. Given that BA interacts with numerous targets within anticancer research frameworks, our findings offer a new avenue for exploring its underlying mechanisms of action. Further investigations are warranted to identify and validate additional targets of BA involved in regulating MM progression.

5 | Conclusions

Our research demonstrates the role of USP13 in promoting MM malignancy and uncovers a novel mechanism of USP13 deubiquitinating PARP1 to stabilize PARP1 protein expression in MM, thereby triggering the DDR of MM cells. More importantly, BA effectively suppresses the growth and progression of MM in vitro and in vivo by targeting USP13/PARP1 signalling, implying its potential application in the treatment of MM solely or in combination with current treatment options.

Author Contributions

Ye Yang: conceptualization, supervision, funding acquisition, writing – review and editing. **Chunyan Gu:** conceptualization, supervision, funding acquisition, writing – review and editing. **Yuanjiao Zhang:** conceptualization, supervision, funding acquisition, writing – review and editing. **Mengjie Guo:** data curation, visualization, writing – original draft. **Han Meng:** manuscript revision. **Yi Sun:** methodology, data curation, visualization. **Lianxin Zhou:** methodology, validation, **Tingting Hu:** methodology, validation. **Tianyi Yu:** methodology, validation. **Haowen Bai:** methodology, validation.

Acknowledgements

This work was supported by National Natural Science Foundation of China 82304599, Scientific Research Foundation of Nanjing University of Chinese Medicine (013091007003-1) (to YZ) and the

Priority Academic Program Development of Jiangsu Higher Education Institutions (Integration of Chinese and Western Medicine).

Conflicts of Interest

The authors declare no conflicts of interest.

Data Availability Statement

The data that support the findings of this study are available from the corresponding author upon reasonable request.

References

1. R. L. Siegel, K. D. Miller, H. E. Fuchs, and A. Jemal, "Cancer Statistics, 2021," *CA: A Cancer Journal for Clinicians* 71 (2021): 7–33.

2. J. L. Kaufman, C. Gasparetto, F. H. Schjesvold, et al., "Targeting BCL-2 With Venetoclax and Dexamethasone in Patients With Relapsed/Refractory t(11;14) Multiple Myeloma," *American Journal of Hematology* 96 (2021): 418–427.

3. G. Zhang, Q. Wang, X. Liu, et al., "An Integrated Approach to Uncover Quality Markers of Traditional Chinese Medicine Underlying Chemical Profiling, Network Target Selection and Metabolomics Approach: Guan-Xin-Jing Capsule as a Model," *Journal of Pharmaceutical and Biomedical Analysis* 190 (2020): 113413.

4. K. Banik, E. Khatoon, C. Harsha, et al., "Wogonin and Its Analogs for the Prevention and Treatment of Cancer: A Systematic Review," *Phytotherapy Research: PTR* 36 (2022): 1854–1883.

5. K. W. Li, Y. Y. Liang, Q. Wang, et al., "*Brucea javanica*: A Review on Anticancer of Its Pharmacological Properties and Clinical Researches," *Phytomedicine: International Journal of Phytotherapy and Phytopharmacology* 86 (2021): 153560.

6. X. Li, C. Liu, X. Zhang, et al., "Bruceine a: Suppressing Metastasis via MEK/ERK Pathway and Invoking Mitochondrial Apoptosis in Triple-Negative Breast cancer," *Biomedicine & Pharmacotherapy = Biomedecine & Pharmacotherapie* 168 (2023): 115784.

7. X. F. Wu, X. H. Wei, Y. Z. Wu, et al., "Progress of Target Determination and Mechanism of Bioactive Components of Traditional Chinese Medicine," *Zhongguo Zhong yao za zhi = Zhongguo Zhongyao Zazhi = China Journal of Chinese Materia Medica* 47 (2022): 4565–4573.

8. P. Zhang, W. Tao, C. Lu, et al., "Bruceine a Induces Cell Growth Inhibition and Apoptosis Through PFKFB4/GSK3beta Signaling in Pancreatic cancer," *Pharmacological Research* 169 (2021): 105658.

9. K. P. Lai, J. Chen, and W. K. F. Tse, "Role of Deubiquitinases in Human Cancers: Potential Targeted Therapy," *International Journal of Molecular Sciences* 21 (2020): 21.

10. Y. Guo, J. Tian, Y. Guo, et al., "Oncogenic KRAS Effector USP13 Promotes Metastasis in non-small Cell Lung cancer Through Deubiquitinating beta-Catenin," *Cell Reports* 42 (2023): 113511.

11. L. Chen, J. Ning, L. Linghu, et al., "USP13 Facilitates a Ferroptosis-To-Autophagy Switch by Activation of the NFE2L2/NRF2-SQSTM1/p62-KEAP1 axis Dependent on the KRAS Signaling Pathway," *Autophagy* 21 (2024): 565–582.

12. B. Zhao, W. Huo, X. Yu, et al., "USP13 Promotes Breast cancer Metastasis Through FBXL14-Induced Twist1 Ubiquitination," *Cellular Oncology* 46 (2023): 717–733.

13. J. Kwon, H. Choi, A. D. Ware, et al., "USP13 Promotes Development and Metastasis of High-Grade Serous Ovarian Carcinoma in a Novel Mouse Model," *Oncogene* 41 (2022): 1974–1985.

14. X. Man, C. Piao, X. Lin, C. Kong, X. Cui, and Y. Jiang, "USP13 Functions as a Tumor Suppressor by Blocking the NF-kB-Mediated PTEN Downregulation in Human Bladder cancer," *Journal of Experimental & Clinical cancer Research: CR* 38 (2019): 259.

15. Z. Qu, R. Zhang, M. Su, and W. Liu, "USP13 Serves as a Tumor Suppressor via the PTEN/AKT Pathway in Oral Squamous Cell Carcinoma," *Cancer Management and Research* 11 (2019): 9175–9183.

16. S. Xiang, J. Fang, S. Wang, B. Deng, and L. Zhu, "MicroRNA-135b Regulates the Stability of PTEN and Promotes Glycolysis by Targeting USP13 in Human Colorectal Cancers," *Oncology Reports* 33 (2015): 1342–1348.

17. P. Tveden-Nyborg, T. K. Bergmann, N. Jessen, U. Simonsen, and J. Lykkesfeldt, "BCPT 2023 Policy for Experimental and Clinical Studies," *Basic & Clinical Pharmacology & Toxicology* 133 (2023): 391–396.

18. P. Tveden-Nyborg, B. Yang, U. Simonsen, and J. Lykkesfeldt, "BCPT Perspectives on Studies Involving Natural Products, Traditional Chinese Medicine and Systems Pharmacology," *Basic & Clinical Pharmacology & Toxicology* 135 (2024): 782–785.

19. C. Gu, W. Wang, X. Tang, et al., "CHEK1 and circCHEK1_246aa Evoke Chromosomal Instability and Induce Bone Lesion Formation in Multiple Myeloma," *Molecular Cancer* 20 (2021): 84.

20. X. Sun, H. Tang, Y. Chen, et al., "Loss of the Receptors ER, PR and HER2 Promotes USP15-Dependent Stabilization of PARP1 in Triple-Negative Breast cancer," *Nature Cancer* 4 (2023): 716–733.

21. A. Ray Chaudhuri and A. Nussenzweig, "The Multifaceted Roles of PARP1 in DNA Repair and Chromatin Remodelling," *Nature Reviews Molecular Cell Biology* 18 (2017): 610–621.

22. M. Guo, D. Sun, Z. Fan, et al., "Targeting MK2 Is a Novel Approach to Interfere in Multiple Myeloma," *Frontiers in Oncology* 9 (2019): 722.

23. J. Heideker and I. E. Wertz, "DUBs, the Regulation of Cell Identity and Disease," *Biochemical Journal* 467 (2015): 191.

24. B. T. Gutierrez-Diaz, W. Gu, and P. Ntziachristos, "Deubiquitinases: Pro-Oncogenic Activity and Therapeutic Targeting in Blood Malignancies," *Trends in Immunology* 41 (2020): 327–340.

25. N. Sarodaya, J. Karapurkar, K. S. Kim, S. H. Hong, and S. Ramakrishna, "The Role of Deubiquitinating Enzymes in Hematopoiesis and Hematological Malignancies," *Cancers* 12 (2020): 1103.

26. P. van den Berk, C. Lancini, C. Company, et al., "USP15 Deubiquitinase Safeguards Hematopoiesis and Genome Integrity in Hematopoietic Stem Cells and Leukemia Cells," *Cell Reports* 33 (2020): 108533.

27. Z. Xiong, P. Xia, X. Zhu, et al., "Glutamylation of Deubiquitinase BAP1 Controls Self-Renewal of Hematopoietic Stem Cells and Hematopoiesis," *Journal of Experimental Medicine* 217 (2020): e20190974.

28. M. Higuchi, H. Kawamura, H. Matsuki, et al., "USP10 Is an Essential Deubiquitinase for Hematopoiesis and Inhibits Apoptosis of Long-Term Hematopoietic Stem Cells," *Stem Cell Reports* 7 (2016): 1116–1129.

29. H. Lei, J. Wang, J. Hu, Q. Zhu, and Y. Wu, "Deubiquitinases in hematological malignancies," *Deubiquitinases in Hematological Malignancies. Biomarker Research* 9 (2021): 66.

30. D. S. Das, A. Das, A. Ray, et al., "Blockade of Deubiquitylating Enzyme USP1 Inhibits DNA Repair and Triggers Apoptosis in Multiple Myeloma Cells," *Clinical Cancer Research: An Official Journal of the American Association for Cancer Research* 23 (2017): 4280–4289.

31. X. H. Chen, Y. J. Xu, X. G. Wang, et al., "Mebendazole Elicits Potent Antimyeloma Activity by Inhibiting the USP5/c-Maf axis," *Acta Pharmacologica Sinica* 40 (2019): 1568–1577.

32. Y. Yao, Y. Zhang, M. Shi, et al., "Blockade of Deubiquitinase USP7 Overcomes Bortezomib Resistance by Suppressing NF-kappaB Signaling Pathway in Multiple Myeloma," *Journal of Leukocyte Biology* 104 (2018): 1105–1115.

33. X. Li, G. Yang, W. Zhang, et al., "USP13: Multiple Functions and Target Inhibition," *Frontiers in Cell and Developmental Biology* 10 (2022): 875124.

34. Q. Wang, Z. Sun, W. Xia, et al., "Role of USP13 in Physiology and Diseases," *Frontiers in Molecular Biosciences* 9 (2022): 977122.

35. P. B. Kanev, A. Atemin, S. Stoynov, and R. Aleksandrov, "PARP1 Roles in DNA Repair and DNA Replication: The Basi(C)s of PARP Inhibitor Efficacy and Resistance," *Seminars in Oncology* 51 (2024): 2–18.

36. G. Tonon, "Myeloma and DNA damage," *Blood* 143 (2024): 488–495.

37. C. Petrilla, J. Galloway, R. Kudalkar, A. Ismael, and F. Cottini, "Understanding DNA Damage Response and DNA Repair in Multiple Myeloma," *Cancers* 15 (2023): 15.

38. W. Kim, F. Zhao, H. Gao, et al., "USP13 Regulates the Replication Stress Response by Deubiquitinating TopBP1," *DNA Repair* 100 (2021): 103063.

39. C. C. Yu, Y. Li, Z. J. Cheng, X. Wang, W. Mao, and Y. W. Zhang, "Active Components of Traditional Chinese Medicinal Material for Multiple Myeloma: Current Evidence and Future Directions," *Frontiers in Pharmacology* 13 (2022): 818179.

40. C. Cipriani, M. P. Pacheco, A. Kishk, et al., "Bruceine D Identified as a Drug Candidate Against Breast Cancer by a Novel Drug Selection Pipeline and Cell Viability Assay," *Pharmaceuticals* 15 (2022): 15.

41. Y. Wang, J. Huang, B. Li, et al., "A Small-Molecule Inhibitor Targeting TRIP13 Suppresses Multiple Myeloma Progression," *Cancer Research* 80 (2020): 536–548.

42. J. Zhang, L. Ai, T. Lv, X. Jiang, and F. Liu, "Asiatic Acid, a Triterpene, Inhibits Cell Proliferation Through Regulating the Expression of Focal Adhesion Kinase in Multiple Myeloma Cells," *Oncology Letters* 6 (2013): 1762–1766.

43. H. Li, X. Zhu, Z. Sun, et al., "Bruceine B Displays Potent Antimyeloma Activity by Inducing the Degradation of the Transcription Factor c-Maf," *ACS Pharmacology & Translational Science* 7 (2024): 176–185.

44. B. C. Valdez, Y. Li, D. Murray, et al., "The PARP Inhibitor Olaparib Enhances the Cytotoxicity of Combined Gemcitabine, Busulfan and Melphalan in Lymphoma Cells," *Leukemia & Lymphoma* 58 (2017): 2705–2716.

45. C. Lu, L. Fan, P. F. Zhang, et al., "A Novel P38alpha MAPK Activator Bruceine a Exhibits Potent Anti-Pancreatic cancer Activity," *Computational and Structural Biotechnology Journal* 19 (2021): 3437–3450.

46. Z. Gao, Y. Zhang, W. Shen, et al., "Bruceine a Inhibited Breast cancer Proliferation and Metastasis by Inducing Autophagy via Targeting PI3K-AKT Signaling Pathway," *Chemical Biology & Drug Design* 103 (2024): e14398.